LUPINE PUBLISHERS

Advances in Robotics & Mechanical Engineering

DOI: 10.32474/ARME.2022.03.000173

ISSN: 2643-6736

Review Article

Effect of Re/Ru on Ingredient Distribution and Creep Property of Nickel-Based Single Crystal Alloys

Tian Songwen[1], Shu Delong[2], Liu lirong[2] and Tian Sugui[2]*

[1]*Shenyang 3D-Dowell Science & Technology Co. LTD, Shenyang, PR China*

[2]*Shenyang University of Technology, Shenyang PR China*

***Corresponding author:** Tian Sugui, Shenyang University of Technology, Shenyang 110870, PR China

Received: August 13, 2022 **Published:** August 25, 2022

Abstract

By means of atom probe tomography (APT) and creeping property testing, the affecting of Re/Re on the element's distribution and creep property of nickel-based single crystal alloy is studied. Results show that the microstructure of alloys consists of cubical *y* and *y* phases, and the most of elements Mo, W, Re, Ru, Cr, Co are dissolved in *y* phase, while the most of Ta, Al, Ni are dissolved in *y* phase. Adding Re/Ru atoms may evidently enhance the creep resistance of alloy, which is ascribed to the Re/Ru making more Al, Ta, Mo, W, Re atoms dissolved in *y* matrix and *y* phase to increase the alloying degree. Particularly, the W, Re, Mo atoms in *y* phase are excluded, during creep, for enriching in g phase near the interface to form their peak content, the lattice distortion from the enriched atoms may hinder dislocations gliding to delay the phase being sheared. The deformed mechanisms of alloy during later creep are the dislocations sliding in *y* phase and shearing *y* phase, the ones of shearing *y* phase may cross-glide from {111} to {001} planes to form the KW locks which may restrain their gliding and cross-gliding to improve the creep resistance of alloy. While the interaction of the Re/Ru with W atoms make some Re, W atoms reserving in *y* phase to delay the diffusing of elements, which may maintain the KW locks from being released to keep the good resistance of alloy.

Keywords: Single Crystal Nickel-Based Alloy; Creep; Concentration Distribution; Deformation Mechanism; KW Locks

Introduction

Single crystal nickel-based alloys consisted of cuboidal γ' phase and γ matrix possess an excellent mechanical and creep properties, and their strength increases with the refractory elements [1,2]. Particularly, adding Re, Ru, W, Mo, Ta may decrease the diffusion rate of elements, wherein, the saturated content of the elements increases from 14.6% (the first-generation single crystal alloys) to 20.7% (the third-generation alloys) [3], which enhances the temperature capacity of alloy about 30°C and 60°C, respectively, by adding 3% and 6%Re [4]. The Re atoms possess a lower diffusion coefficient in nickel alloy [5], especially, these atoms may form the atomic cluster to enrich in γ phase [6] for impeding dislocations gliding. But the precipitation of TCP phase occurs in alloys with the increase of Re content [7], which decays the strength and resistance of alloys [8]. This is ascribed to some refractory elements being consumed due to TCP precipitated from γ phase. Moreover, the initiation and propagation of cracks occur easily, during creep of alloys, due to the stress concentration being easily caused by TCP phase [9]. The element Ru can effectively inhibit the precipitation of TCP phase in Re-containing single crystal alloys to enhance their creep resistance at elevated temperature [10,11]. And appending 3% and 5%Ru atoms in 6%Re alloys become the principal features of the fourth and fifth generation alloys due to the action of Ru atoms enhancing the resistance of alloys [12]. On one hand, the Ru atoms make the rafted γ' structure being more regularized and integrated during creep [10]. For one thing, the Ru atoms may increase the γ/γ' mismatch to abate the nucleating rate of TCP phase [11]. Thus, the Ru may greatly enhance the alloying degree of elements, which make the alloys displaying an excellent creep resistance. Consequently, the microstructure and creep behavior of Re/Ru alloys are widely investigated [13]. But the literatures declare [14,15] that no obvious effect is revealed on the Ru improving the elements distribution of γ/γ' phases [16], which hints that the cause of Ru restraining TCP precipitation is still an open problem. Furthermore, the effect of Re, Ru improving the elements distribution of alloy needs to be investigated.

The deformation features of Re/Ru-containing alloys during creep at 1100°C is the dislocation pairs shearing γ' phase [17]. And the reason of alloys displaying different creep lives is attributed to the various strength and volume fraction of γ' phase [18]. Moreover, it is considered that the reason of nickel-based alloys exhibiting the excellent mechanical and creep property is related to the anomalous yield strength of Ni3Al phase [19], which is attributed to forming the KW locks by the cross-gliding of dislocations [20]. And it had been reported that the better creep resistance of both Ni3Al single crystal at 700°C [21] and 2%Re Ni-based alloy at 980°C [22] is related to the formed KW locks. But if the KW locks can be formed and retained in the Re/Ru-containing alloys during creep at 1080°C is still unclear. Even though the microstructure and creep property of the Re/Ru-containing alloys had been investigated [23,24], the effect of the element's distribution on the deformation features of alloys at high temperature is not clear. Hereby, in the paper, the Re/Ru-free and 4.5%Re/3.0%Ru single crystal alloys were prepared, passing through the creep property testing at 1080°C and microstructure observation, to reveal the distributing feature of elements in alloys under atom probe technology (APT), so that the affecting of Re/Ru on the distributing feature and creep behavior of alloy is studied.

Experimental Procedure

Two master alloys with Re/Ru-free and 4.5%Re/3.0%Ru composition features were, separately, made into the single crystal bars with [001] orientation by selecting crystal method in a vacuum directional solidification furnace, all bars are within 7^0 diverging from [001] orientation. For convenient description, the Re/Ru-free and 4.5%Re/3.0%Ru alloys are defined as Alloy 1 and Alloy 2, separately. The compositions of two alloys are Ni-Al-Ta-Cr-Co-Mo-W and Ni-Al-Ta-Cr-Co-Mo-W-4.5%Re-3.0%Ru (mass fraction, %). For the bars, the solution treatment of grading heated is used to avoid the incipient melting of eutectic microstructure having lower melting point. Therefore, the heat treatment process of Alloy 1 and Alloy 2 are given as follows: 1)1300°C × 2h+1310°C × 6h, AC. + 1080°C × 4h, AC. +870°C × 24h, AC. 2)1310°C × 2h+1320°C×15h+1325°C×10h + 1328°C × 5h, A.C.+1150°C × 4h, A.C.+870°C × 24h, A.C. After heat treated and crept, the single crystal bars of two alloys are processed into, respectively, the needle-like specimens of 0.3 mm × 0.3 mm and length of 14 mm along [001] orientation. The specimens are, separately, placed in the atom probe with LEAP4000XHR model for detecting the elements distribution of alloys by atom probe tomography (APT). In the period of survey, it is necessary to cool the specimens to 20-80 K, under super high vacuum (UHV), for reducing the atoms' thermal vibration. The specimens are joined to the anode so that keeps the atom being activated on the top, and the mass/electric charge ratio of vaporizing ions is surveyed by mass spectrograph, which may identity the mass peak and kinds of atoms to obtain the 3D mapping of the elements further. The used method in 3D atom probe tomography were described in the literature [25]. And the IVAS 3.6.8 software is used to make the date analysis.

After reconstructed by APT, the mapping of Al and Cr atoms in two alloys are indicated in Figure 1, which labels the sizes of distributing mapping. Because of the most of Al, Cr atoms being dissolved in γ' and γ phases, separately, the enriched zones of Al, Cr atoms are defined as γ' and γ phases, separately. In 3DAP mapping, the columnar ROIs (region of interest) with the size of ϕ 10nm x 20nm are chosen in the zone near γ/γ' interface to evaluate the affecting of Re/Ru on the element's distribution of alloys. After heat treated, the bars with single crystal are processed to make the specimens having the sizes of 4.6 mm x 2.6 mm and gauge length of 22 mm. The specimens were placed in the creep testing machine (model of GWT504) to survey the creep property of alloys at 1080°C/137MPa. The microstructure of alloys is observed under SEM and TEM to study the affecting of Re/Ru on the content distribution and creep property of alloy.

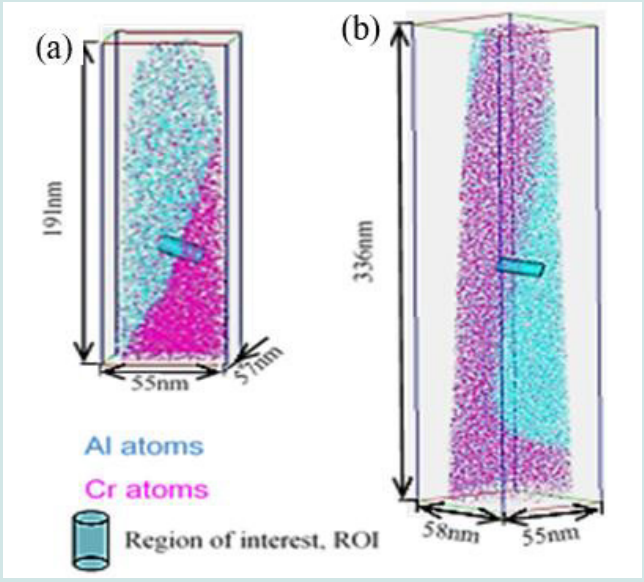

Figure 1: Reconstructed 3D distribution mapping of atoms and ROIs of the alloys by APT. (a) Alloy 1, (b) Alloy 2.

Experimental Results and Analysis

Microstructure and Creep Properties

The cubical γ' and γ phases constitute microstructure of two alloys after heat treated, wherein the cubical γ' phase arrays regularly along <100> orientation, as shown in Figure 2. But the slight difference on the size of cubical γ' phase appears in two alloys, such as, the size of about 0.44-0.47 μm is surveyed in Alloy 1, while the size of about 0.38-0.40 μm is surveyed in Alloy 2. Moreover, the sizes of γ channels arranged along the horizontal and upright directions are about 0.1-0.2 μm, while the volume fractions of γ' phase in Alloy 1 and Alloy 2 are surveyed to be about 64% and 68%, separately, by extraction technology. The creep curves of two alloys at 1080°C/137MPa are surveyed, as shown in Figure 3, indicating that the creep rate of Alloy 1 during steady state is 0.016%/h, the creep life of 238 h is surveyed. While the creep rate of 0.0066%/h is surveyed during steady state of Alloy 2, its lifetime is 486h. Consequently, it is concluded that the 4.5%Re/3.0%Ru alloy possesses a lower strain rate and longer life during creep. Wherein, the lifetime of alloy after adding Re/Ru elements are enhanced to about 104.2%. As the creep continues, the creep rate of alloy decreases for entering steady state stage under the action of strain strengthening. The diffusing theory considers [26] that the void diffusing controls the creep of alloys at high temperature, especially, the higher void concentration being located in the γ/γ' interfaces promote 's the diffusion of atoms along interfaces, which causes the occurrence of alloys straining along stress axis. Therefore, the strain rate of alloys may be expresses as:

$$\dot{\varepsilon} = \frac{D}{kT} \cdot \frac{\sigma . b^3}{2d^2} = A \frac{D . \sigma . \Omega}{k . T . d^2} \qquad (1)$$

Here, D self-diffusion coefficient, k Boltzmann constant, A a constant, d the size of γ' phase, $\Omega = b^3$ the volume of atoms migration. Consequently, the raised loading may accelerate the alloy' strain rate, but the rate is inversely proportional to the square of γ' size. Hence, compared to Alloy 1, the Alloy 2 exhibits a lower creeping rate and longer lifetime due to the smaller diffusion coefficient (D) and migration volume of atoms during creep.

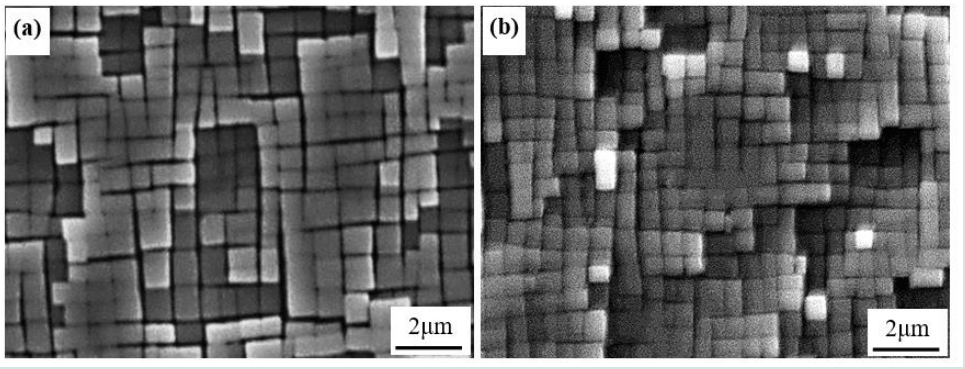

Figure 2: Morphologies of alloys after fully heat treatment (a)Re/Ru-free alloy, (b)4.5%Re/3.0%Ru alloy.

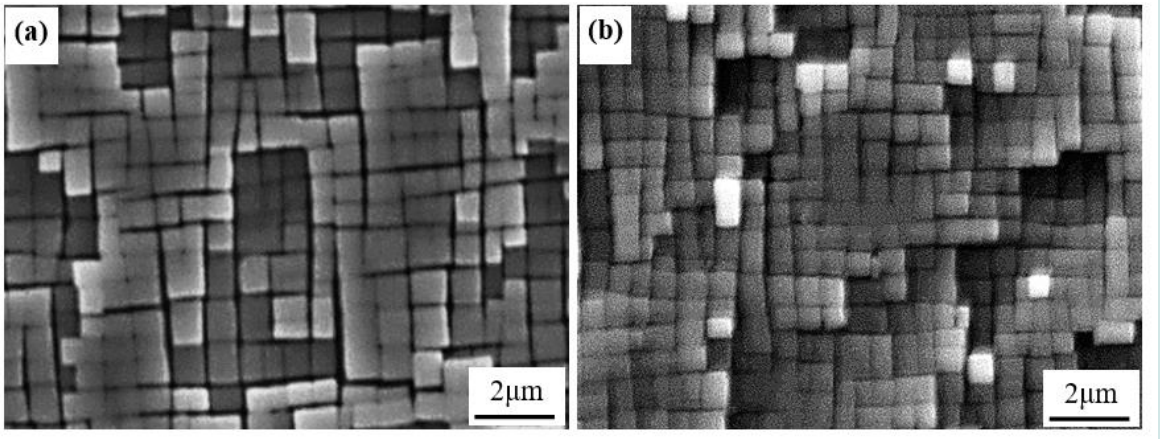

Figure 3: Creep curves of the alloys at 1080°C/137MPa.

Influence of Re/Ru on Distribution of Elements

The average content distributions (atom fraction, at%) of atoms Al, Ta, Mo, W, Cr, Co, Re, Ru in γ and γ' phases of two alloys are surveyed by APT, as shown in Table 1. This indicates that the most of Al, Ta, Ni atoms are dissolved in γ' phase, so the ones are the former of γ' phase, while the most of Cr, Co, Mo, W, Re, Ru atoms are dissolved in γ phase, the ones are the former of γ phase [25-27]. And a bigger content difference of some elements is designed in two alloys, such as, the Mo content of 6% and 3% (mass fraction, %) are designed, respectively, in Alloy 1 and Alloy 2. Consequently, the ratio ( ) of the atoms Me in γ/γ' phases is used for convenient comparison, Where the number 1 is defined as the radix of atoms with lowest content, the content of atoms with higher content is defined as the multiple of the ones with lower content [25], the ratios of the elements in γ/γ' phases are calculated, as listed in Table 1. Table 1 provides that the amounts of atoms in phase of Alloy 1 and Alloy 2 are 42.36at. % and 37.26at.%, separately, while the values of 29.49at% and 31.72at% corresponds, separately, the ones of γ' phase. The ratios of atoms in γ/γ' phase of two alloys is about 1/1.43 and 1/1.18, separately. Although the γ phase contains the most of atoms Re, Ru, the ratio of Re/Ru making other atoms in γ/γ' phases increase. Consequently, it is concluded that the distribution of various elements in γ' phase may be improved by adding Re/ Ru atoms.

The columns (Region of interest, ROI) of φ 10nm x 20nm are chosen, in the mapping of atoms concentration, to identify easily γ' and γ phases, as shown in Figure 1. Wherein, the images of Al enriched in the ROIs of two alloys are shown in Figure 4(a),4(b), though the same content of Al atoms is added in two alloys, the various content of Al atoms display in γ/γ' phases of alloys, as shown in Figure 4(a). For the Re/Ru-free Alloy 1, the atomic fractions of Al dissolving in γ' and γ phases are surveyed to be 18.81 at% and 2.72 at%, separately, the ratio of Al dissolved in γ' and g phases is 6.92/1, as shown in Figure 4(a) and Table 1. After adding 4.5%Re/3.0%Ru, the contents of the Al in γ' and γ phases of Alloy 2 are identified to be 18.12 at% and 3.56 at%, respectively, and the ratio of Al dissolved in γ/γ' phases of Alloy 2 is 5.08/1, which is given in Table 1 and Figure 4(b). Consequently, it is concluded from the data that the Re, Ru atoms may promote much more Al atoms dissolving in g phase to improve the distributing feature of elements in g and γ' phases [25]. In the mapping of atoms in γ/γ' phases, the size of ϕ 10nm x 20nm is chosen in the Region of Interest (ROI) near γ/γ' interface for drawing the outlines of elements, the outlines in the region near interface are constructed by the average contents of the atoms in γ,γ' phases. Here, the outlines of atoms Al, Re, Ru, Mo and W in the zone near interface are indicated in Figure 5. Wherein, the content curves of elements Al in Alloy 1 and Alloy 2 are labeled by the numbers 1 and 2 in Figure 5(a), and the content of the element Al C_{Al} =10 at. % is defined as the "0" point in the horizontal coordinate. Therefore, the left side region of the "0" point in horizontal coordinate is distinguished as γ' phase, the right-side region of the "0" point in the one is distinguished as γ matrix. It is indicated from Figure 5(a) that, although two alloys design the same Al content, the γ,γ' phases in Alloy 1 and Alloy 2 display the various contents of Al atoms. And the element Ta displays also a similar feature of distribution. According to the definition of phase composition [28], the contents of the element Al C_{Al} = 90% ${}^{0}C_{Al}^{\gamma'}$ and C_{Al} = 110% ${}^{0}C_{Al}^{\gamma}$ are defined as the composition points of γ' *and* γ phases, respectively, (${}^{0}C_{Al}^{\gamma}$ *and* ${}^{0}C_{Al}^{\gamma'}$ and are the average contents of Al in γ *and* γ' phases, respectively, as indicated in Table 1. And the region between the composition points is defined as the transition zone between γ *and* γ' phases. It is indicated from Figure 5 that the size of the transition zone in two alloy is measured to be 2 nm (from -1.0 nm to 1.0 nm). The average contents of atom Cr in γ *and* γ' phases of Alloy 2 are determined to be 8.34 at% and 1.17 at%, and the ratio of Cr atom in γ *and* γ' phases is 1/7.13, as shown in Table 1. The outlines of Ru, Ru atoms distributing in the ROIs of Alloy 2 is expressed in Fig. 5(b). Because the most of Re, Ru atoms are dissolved in γ phase, and the ratios of atoms Re and Ru dissolving in γ'/γ phases of Alloy 2 are about 1/5.02 and 1/3.86, respectively, thus, the content of Re in γ' phase is slightly increased by adding Ru [25]. The average contents of Re in γ' *and* γ phases of Alloy 2 are identified to be about 0.71 at% and 3.56 at%, respectively, consequently the bigger content gradient of Re maintains still in the interface zone, as labeled in Figure 5(b). Furthermore, the average contents of Ru in γ' *and* γ phases are identified as 0.81at. % and 3.13at%, so the bigger content gradient of Ru atoms maintains still in the ROI, as labeled by the outline of Ru. The distribution curves of the W and Mo atoms in two alloys are shown in Figures 5c & 5d, indicating that the W atoms are uniformly distributed in γ/γ' phases, as labeled by the black curve of Figure 5(d). Although the most of Re/Ru and Mo atoms are distributed in γ phase, the various ratios of Re, Ru, Mo atoms in γ/γ' phases are identified to be 1/5.02, 1/3.86 and 1/2.44, separately, as shown in Table 1. Compared to Alloy 1, the ratios of Mo in γ'/γ phases of Alloy 2 diminish from 1/5.37 to 1/2.44, as indicated in Table 1, indicating that much more Mo atoms may be dissolved in γ' phase by adding Re/Ru. Similar to the distributions of Mo in two alloys, compared to Alloy 1, the ratio of W atoms in γ'/γ phases of Alloy 2 change from 1/4.51 to 1/1.17, as indicated in Table 1, because the Re/Ru enhance and decrease the content of W in γ' *and* γ phases, separately. This hints that adding Ru, Re atoms may improve the distribution of W in γ'/γ phases. Furthermore, compared to in Alloy 1, the ratios of atoms Ta, Cr, Co in γ'/γ phases of Alloy 2 are slightly diminished by adding Ru, Re atoms, as shown in Table 1. The outlines and gradients of Al, Re/Ru, Mo and W atoms distributing in γ'/γ phases of two alloys are indicated in Figure 5, wherein, the bigger gradients of Al, Mo, W atoms in γ'/γ phases display in Alloy 1, as shown in Figures 5(a, c, d). Here the outlines of Co, Cr atoms in γ'/γ phases are omitted because the ones are similar to the distribution of Mo. Compared to Alloy 1, the outline gradient of Al distributing in γ'/γ phases of Alloy 2 decreases greatly, as labeled in the curve 1 of Figure 5(a), therefore, the decreased content of Al in γ' phase and increased one in γ phase may be realized by adding Re/Ru. Furthermore, the contents of Mo in Alloy 1 and Alloy 2 are designed to be 6.0 wt.% and 3.0wt%, respectively, thus the Mo content in Alloy 2 displays a lower content and ratio, as shown in Figure 5(c).

Table 1: Distribution and ratios of elements in γ/γ¢ phases of two alloys (Atomic fraction, at.%).

	Regions	Al	Ta	Mo	W	Cr	Co	Re	Ru	Total
Alloy 1	γ phase	2.72±0.1	0.46±0.1	8.22±0.4	2.80±0.2	16.51±1	11.65±0.4	0	0	42.36
	γ' phase	18.81±0.4	3.82±0.2	1.53±0.2	0.62±0.2	1.76±0.2	2.95±0.2	0	0	29.49
	Ratio	6.92/1	8.31/1	1/5.37	1/4.51	1/9.39	1/3.95	-	-	1/1.43
Alloy 2	γ phase	3.56±0.2	0.60±0.2	3.42±0.2	1.96±0.2	8.34±0.2	12.69±0.4	3.56±0.2	3.13±0.2	37.26
	γ' phase	18.12±0.4	3.77±0.2	1.40±0.2	1.68±0.2	1.17±0.1	4.06±0.2	0.71±0.1	0.81±0.1	31.72
	Ratio	5.08/1	6.28/1	1/2.44	1/1.17	1/7.13	1/3.13	1/5.01	1/3.86	1/1.18
Alloy 2 After crept	γ phase	3.31	--	--	1.91	5.58	11.14	3.57	3.36	32.92
	γ' phase	14.94	--	--	1.65	0.78	3.7	0.42	0.86	27.41
	Ratio	4.51/1	6.55/1	1/2.62	1/1.15	1/7.15	1/3.09	1/8.50	1/3.91	1/1.20

Note: "--" in the Table is not suitable for public element concentration

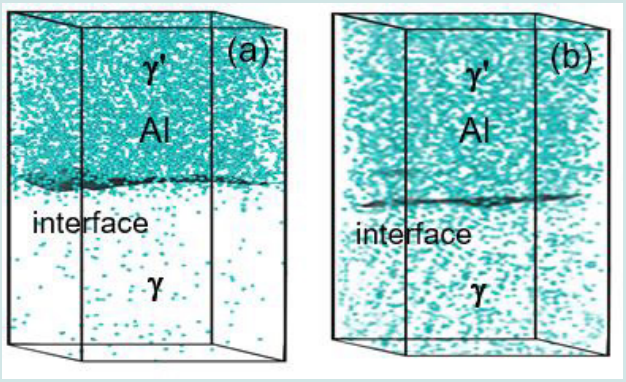

Figure 4: Atomic distribution of Al atoms in / phases of superalloys (a) Al mapping in Alloy 1, (b) Al mapping in Alloy 2.

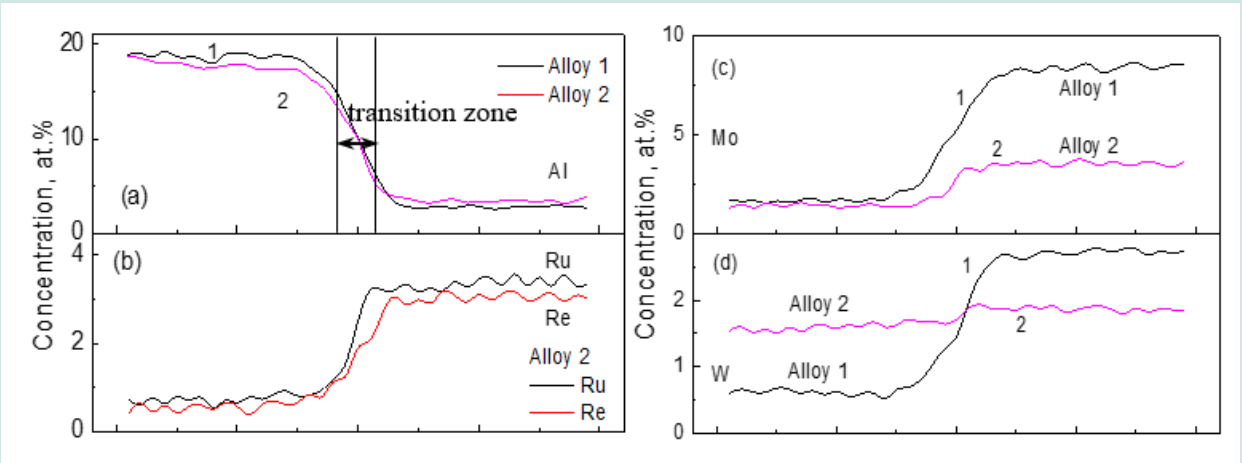

Figure 5: Distribution of elements in the region of interest (ROI) of two alloys (a) Al, (b) Re and Ru, (c) Mo, (d) W.

Influence of Creep on Distribution of Elements

After creeping, the content mapping of Ta and Co atoms in Alloy 2 are shown in Figures 6a & 6b, in which the enriching zones of the atoms Ta, Co are located in the up and down sides, separately. Similar to the element Al, the element Ta is a γ' former, therefore, the enriched zone of Ta atoms is identified as γ' phase, while the enriched zone of Co atoms is identified as g phase. But some fine particles of enriched Al are precipitated in γ matrix of Alloy 2 after

crept for 486 h up to fracture at 1080 °C/137MPa, as indicated in the downside of Figure 6(a). The size of fine enriching Al particles is about 10nm, the interval of the enriching Al particles in γ phase far from the interface of γ' phase is about 15nm. After creeping, the average content (at.%) of elements in γ/γ' phases of Alloy 2 are measured by 3D APT, as shown in the down part of Table 1. Although the measured error of the elements content may occur, the effect of high temperature creep on the content distribution of elements may be evaluated according to the ratio of elements in γ/γ' phases. The total atomic fractions of elements in the γ, γ' phases of Alloy 2 before creep are measured to be 37.26 at.% and 31.72 at.%, respectively, and the most of Re, Ru atoms are dissolved in the γ phase of Alloy 2 . After creeping for 486 h at 1080°C/137MPa, the total atomic fractions of elements in γ, γ' phases of Alloy 2 are surveyed to be 32.92 at.% and 27.41 at.%, respectively, as shown in Table 1. Particularly, the average contents of the Al atoms in γ, γ' phases of Alloy 2 before/after creep decrease from 3.56at%, 18.12at% to 3.31at%, 14.94at %, separately, and the data of Cr distributing in γ, γ' phases of Alloy 2 displays also a similar feature, as shown in Table 1. This is related to the spoilage of atoms Al, Cr being oxidized during creep [27].

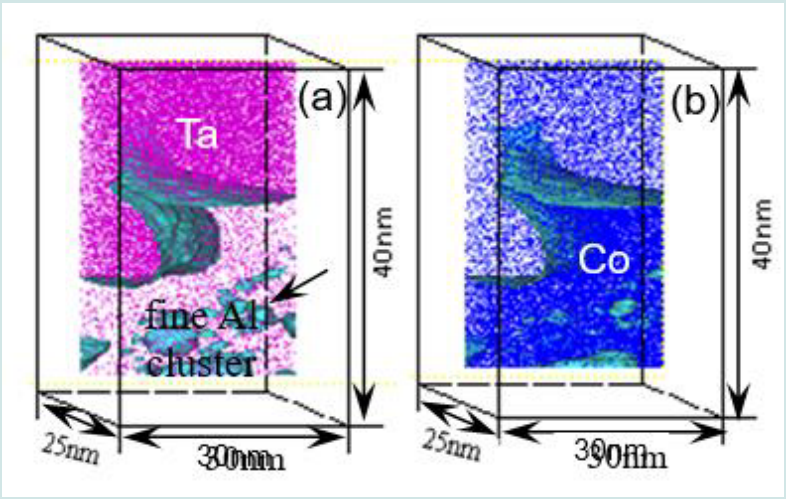

Figure 6: Atomic distribution of Al in' Y/Y phases of Alloy 2 (a) Ta mapping in Alloy 2 after crept, (b) Co mapping in Alloy 2 after crept.

After Alloy 2 is crept for 486 h at 1080oC/137MPa, the outlines of Re, W, Mo, Ru atoms in the zone near interface are expressed in Figure 7. Compared to before crept, no obvious change of the concentrations and ratios of W, Mo and Co atoms in γ/γ' phases occur after crept, as indicated in Table 1. Wherein, the concentration of Re dissolved in γ' phase diminishes from 0.71at.% to 0.42at.%, the ratios of Re dissolved in γ'/γ phases diminishes from 1/5.02 to 1/8.50, which depends on the strong binding force of Ru with the adjacent atoms [25]. It is considered by analysis that the hybridization in the d orbit electronic shell of the Ru with Re, W atoms increases the binding force between them [29]. During creep, the hybridization of the Ru with Re, W atoms make the ones hard to diffuse long-range, so that the ones may stably exist in γ/γ' phases. Moreover, the Re atom in γ' phase may be excluded, as the creep continues, due to the lower solubility of Re in γ' phase [25], which is considered to be one of the reasons for decreasing content of Re in γ' phases after Alloy 2 is crept up to fracture. After crept, the outlines of W, Ru, Re and Mo atoms in γ/γ' interface area is labeled in Figure 7, the size of the transition area between γ *and* γ' phases are measured to be about 3.8 nm (from -1.0 to 2.8 nm). Moreover, Figure 7 indicates the peak values of W, Re, Mo content appear in γ phase close the transition area. Wherein, the peak concentrations of the W, Mo atoms are smaller, the peak concentration of Re atoms is larger, as labeled by the arrow in Figure 7, which is related to the coarsening of γ' phase and redistribution of elements during creep. As the creep continues, the W, Re, Mo atoms in γ' phase are excluded for enriching in γ phase near the interface due to the low solubility of Re in γ' phase. On the one hand, the directional coarsening of γ' phase in alloy occurs, and the atoms W, Re, Mo and Ru in γ' phase are excluded for migrating to the γ phase near interface according to the balance principle of atoms in γ/γ' phases. On the other hand, the atoms are hard to diffuse long-range in γ phase due to their low diffusion coefficient, therefore, the W, Re and Mo atoms may be enriched in the zone close interface. This is considered to be one of the reasons for Re reducing ratio from 1/5.02 to 1/8.50. Furthermore, after crept, the content distribution of the Ru atoms in alloy is similar to the one of Al, Co atoms (peak curves are omitted), no peak content of the Ru atoms is detected in γ phase near interface. This is attributed to that the Ru atoms are easily for long-range diffusing, due to the big diffusion coefficient of the ones in Ni matrix, to prevent from their segregation during creep. Because much more refractory elements are dissolved in Alloy 2, the γ *and* γ' phases in alloy maintain an excellent ability of resistance creep, and the critical shearing stress (τ_c) of dislocations shearing γ' phase is expressed as follows [30] :

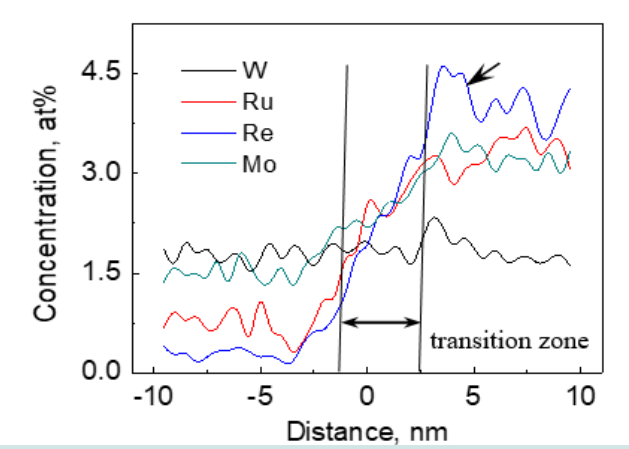

Figure 7: Concentration curves of W, Ru, Re and Mo atoms in the γ, γ′ phases of alloy after crept.

$$\tau_c = \frac{B.\mu.(\Delta\alpha)}{b}\left(\frac{c_T.r.f.\eta_{APB}}{T}\right)^{1/2} \quad (2)$$

Here, B a constant, μ the shear modulus, b Burger's vector of dislocation, η APB the APB energy of unit area, T the line tension, $\Delta\alpha$ the mismatch of γ'/γ phases. The equation (2) indicates that the critical shear stress (τ_c) of dislocations cutting γ' phase may increase with the volume fraction, size of γ' phase and refractory elements. Hence, Alloy 2 keeps a better resistance of creep due to the higher amounts of γ' phase which dissolves much more refractory elements.

Effect of Re/Ru on Deformation Feature

The deformed feature of Alloy 1 crept for 238 h up to rupture is shown in Figure 8, wherein, the deformed feature in some zones is indicated in Figure 8 (a). It is understood from Figure 8 (a) that γ' phase in alloy has transformed into the rafted structure, and dislocation networks distribute in γ'/γ interfaces. Although a few dislocations appear in the zone A, some dislocations had sheared rafted γ' phase, as indicated in the zone B. In addition, the contorted configuration of rafted γ'/γ phases display in the zone A, which is ascribed to their bigger strain [27]. The configuration in the zone near fracture of alloy crept up to rupture, as indicated in Figure 8(b), the direction of the applied stress are labeled by the arrows, the rafted γ'/γ phases in the local zone display the contorted configuration, as labeled in the zone C. Wherein, a great deal of dislocations are slipping in the γ matrix, as indicated in the zone D, and the trace direction of dislocation gliding in γ matrix is about 45° angle along loading direction, which corresponds the max shearing stress. Moreover, the denser dislocations are distributed in the γ'/γ interfaces, as indicated in the zone E of Figure 8(b). The fact that some dislocations shear γ' phase hints the zone having lost resistance of creep.

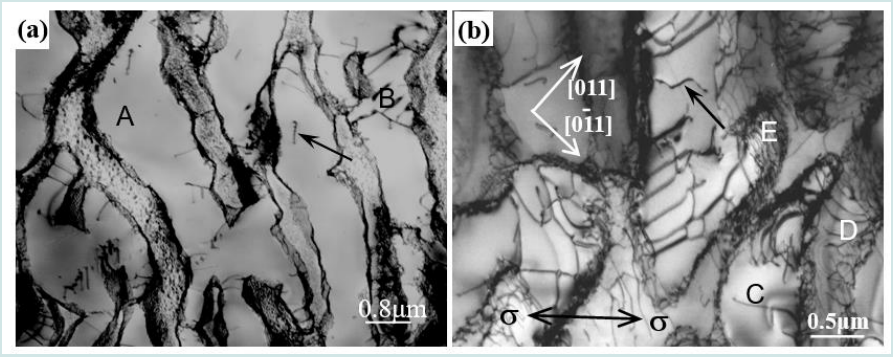

Figure 8: Deformation feature of γ′/γ phases in Alloy 2 crept for 238h up to fracture at 1080°C/137MPa (a) Microstructure in some regions, (b) microstructure in the region near fracture.

It is analyzed and considered according to Figure 8(b) that the deformed characteristics of alloy during creep are dislocations gliding in g matrix and shearing rafted γ' phase. The main/second gliding dislocations are alternately activated as the creep continues [27], the main gliding system of ones is firstly activated, and then the second gliding dislocations is activated, and the main/second gliding dislocations are alternately activated to shear rafted γ'/γ phases[20, 22], so that the contorted of rafted γ'/γ phases occurs.

Further, the contorted of rafted γ'/γ phases increase with strain of alloy, which promotes the initiation and propagation of cracks along γ'/γ interface. This is thought to be the damaging characteristics of alloy during creep. The microstructure of the 4.5%Re/3%Ru Alloy 2 crept for various time at 1080°C/137MPa is shown in Figure 9. Figure 9(a) is a configuration of the alloy after crept for 50h, which verifies that the γ' phase in alloy has changed into the N-type rafted structure. And some networks are piled up in the γ'/γ interfaces due to its bigger mismatch, as expressed in the square frame of Figure 9(a). During creep, some dislocations glide to γ'/γ interface to react with the networks, which may change the gliding direction to promote the dislocations climbing over the rafted γ' phase. The magnified image of the zone is exhibited in the downside of Figure 9(a). Moreover, a great number of dislocations are gliding in the g matrix for displaying in the region F, but no dislocation is detected in the rafted γ' phase. The microstructure of Alloy 2 crept for 200h is shown in Figure 9(b), although the slight distorted image of rafted γ' phase exhibits in the zone, the orientation of rafted γ' phase is still perpendicular to stress axis, and the trace of dislocations shearing γ' rafts is about 45° angles of loading direction [20], as remarked by the short arrow in Figure 9(b). Furthermore, the size of γ channels is about 0.1-0.2 μm, and the regular dislocation networks distribute in the γ'/γ interfaces, as labeled by the longer arrow. After creeping for 486h up to rupture, the microstructure in the zone near fracture is expressed in Figure 9(c), which indicates that the width of g matrix channels has increased from 0.1-0.2 μm to 0.3-0.4 μm. Wherein, the traces of dislocations shearing γ' rafts are about 45° angles (<011>) relative to the stress axis [20], as remarked by the arrows in Figure 9(c). And the dislocations with <011> trace in γ' phase display the various characteristic because of the bigger twisted degree of rafted γ'/γ phases. Moreover, the Burgers vector of dislocations shearing γ' phase identified as <110> super-dislocation and (1/2)<110> partials which may slip in the (111) or (100) planes [20-27]. Wherein, the Burgers vector of dislocation trace with double lines feature is identified as b = (1/2)<110> and located in (100) plane [20-22]. Therefore, the dislocation configuration is known as the KW locks coming from the cross-slipping of super-dislocation form {111} to {100} planes, the one may be decomposed to shape the configuration of (1/2)<110> partials plus anti-phase boundary (APB), as remarked by the vertical arrow in Figure 9(c). Therefore, the 4.5%Re /3%Ru alloy at high temperature displays an outstanding creep resistance because the KW locks formed during creep may restrain their gliding and cross-gliding.

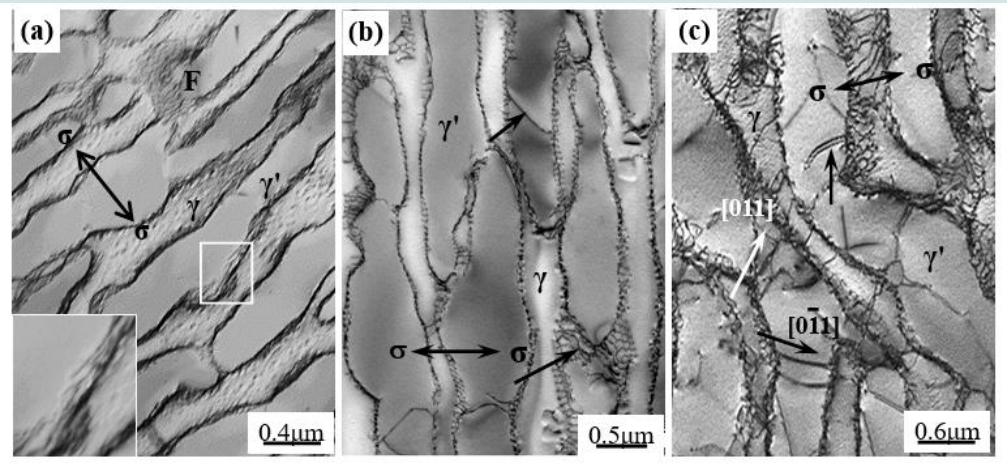

Figure 9: Microstructures of 4.5%Re/3%Ru alloy crept for different times at 1100°C/137MPa (a) Crept for 50h, (b) crept for 200h, (c) crept for 486h up to fracture.

Conclusion

a. The microstructure of alloys consists of cubical γ' and γ phases, and the most of Al, Ta, Ni are dissolved in γ' phase, while the most of Co, Cr, Mo, W, Re, Ru are dissolved in γ phase, the atoms are distributed in γ/γ' phases of two alloys according to various ratios.

b. Adding Re/Ru may evidently enhance the ability of alloy resisting creep, and the lifetime of alloy may be enhanced from 238h to 486h under 1080oC/137MPa. Wherein, the Re, Ru may promote more Al, Ta, Mo, W atoms dissolving in γ matrix and γ' phase, respectively, to increase the alloying degree of γ and γ' phases, which is one of the reasons of the alloy displaying the better creep property.

c. The W, Re, Mo atoms in γ' phase may be excluded, during creep, for enriching in g phase near the interface to form their peak content, the lattice distortion coming from the enriched Mo, W, Re atoms may hinder dislocations gliding to delay the γ' phase being sheared. Wherein, the Re atom with lower diffusion coefficient may delay the diffusing of Mo, W atoms from γ' phase to maintain their higher content.

d. The deformed characteristics of alloy during later creep is the dislocations gliding in γ phase and shearing γ' phase, the

ones of shearing γ' phase may cross-glide form {111} to {100} planes to form the KW locks for inhibiting their gliding and cross-gliding to improve the creep resistance of alloy.

e. The interaction of the Ru and Re, W atoms make some Re, W atoms reserving in γ' phase to delay the diffusing of elements in alloy, which may maintain the KW locks from being released at high temperature to keep the good resistance of alloy in the later period of creep.

Acknowledgements

Sponsorship of this research by the National Natural science foundation of China under grant no. 51271125 is gratefully acknowledged.

References

1. Nystrom JD, Pollock TM, Murphy WH (1997) Discontinuous cellular precipitation in a high-refractory nickel-base superalloy. Metallurgical & Materials Transactions A 28(12): 2443-2452.
2. Yeh AC, Sato A, Kobayashi T (2008) On the creep and phase stability of advanced Ni-base single crystal superalloys. Materials Science and Engineering A 490(1): 445-451.
3. Blavette D, Caron P, Khan T (1986) An atom probe investigation of the role of rhenium additions in improving creep resistance of Ni-base superalloys. Scripta Metallurgica 20(10): 1395-1400.
4. Acharya MV, Fuchs GE (2004) The effect of long-term thermal exposures on the microstructure and properties of CMSX-10 single crystal Ni-base superalloys. Mater Sci Eng A 381(1-2): 143-153.
5. Muller L, Glatzel U, Felle Kniomeeier M (1992) Modelling thermal misfit stress in nickel-base superalloy containing of high-volume fraction of γ phase. Acta Metallurgica & Materialia 40(6): 1321-1327.
6. Carroll L J, Feng Q, Pollock T M (2008) Interfacial dislocation networks and creep in directional coarsened Ru-containing nickel-base single crystal superalloys. Metall. Trans. A 39(6): 1290-1307.
7. Zhang JX, Murakumo T, Harada H (2003) Dependence of creep strength on the interfacial dislocations in a fourth generation SC superalloy TMS-138. Scripta Materialia 48(3): 287-293.
8. Zhao K, Ma YH, Lou LH (2005) μ phase in a nickel base directionally solidified alloy. Materials Transactions 46(1): 54-58.
9. Mackay RA, Gabb TP, Nathal MV (2013) Microstructure-sensitive creep models for nickel-base superalloy single crystals. Materials Science & Engineering A 582(10): 397-408.
10. Tan XP, Liu JL, Jin T (2011) Effect of ruthenium on high-temperature creep rupture life of a single crystal nickel-based superalloy. Materials Science & Engineering A 528(29): 8381-8388.
11. Reed RC, Yeh AC, Tin S (2004) Identification of the partitioning characteristics of ruthenium in single crystal superalloys using atom probe tomography. Scripta Materialia 51(4): 327-331.
12. Yeh AC, Tin S (2006) Effects of Ru on the high-temperature phase stability of Ni-base single-crystal superalloys. Metallurgical & Materials Transactions A 37(9): 2621-2631.
13. Geng CY, Wang CY, Yu T (2004) Site preference and alloying effect of platinum group metals in γ' -Ni3Al. Acta Materialia 52(18): 5427-5433.
14. Matuszewski K, Müller A, Ritter N (2015) On the thermodynamics and kinetics of TCP phase precipitation in Re- and Ru-containing Ni-base superalloys. Advanced Engineering Materials 17(8): 1127-1133.
15. Cui CY, Osawa M, Sato A (2006) Effects of Ru additions on the microstructure and phase stability of Ni-base superalloy, UDIMET 720LI. Metallurgical & Materials Transactions A 37(2): 355-360.
16. Yokokawa T, Osawa M, Nishida K (2003) Partitioning behavior of platinum group metals on the γ and γ' phases of Ni-base superalloys at high temperatures. Scripta Materialia 49(10): 1041-1046.
17. Zhang JX, Wang JC, Harada H (2005) The effect of lattice misfit on the dislocation motion in superalloys during high-temperature low-stress creep. Acta Materialia 53(17): 4623-4633.
18. Hemker KJ, Mills MJ, Nix WD (1991) An investigation of the mechanisms that control intermediate temperature creep of Ni3Al. Acta Metallurgica Et Materialia 39(8): 1901-1913.
19. Cairney JM, Rong TS, Jones IP (2003) Intermediate temperature creep mechanisms in Ni3Al[J]. Philosophical Magazine 83(15): 1827-1843.
20. Tian SG, Zhang BS, Shu DL (2015) Creep properties and deformation mechanism of the containing 4.5Re/3.0Ru single crystal nickel-based superalloy at high temperatures. Materials Science and Engineering A 643: 119-126.
21. Heckl A, Neumeier S, Göken M (2011) The effect of Re and Ru on γ/γ' microstructure, γ-solid solution strengthening and creep strength in nickel-base superalloys. Mater Sci Eng A 528: 3435-3444.
22. Tian SG, Wu J, Shu DL (2014) Influence of element Re on deformation mechanism within γ' phase of single crystal nickel-based superalloys during creep at elevated temperatures. Mater. Sci. Eng., A 616: 260- 267.
23. Zhang JX, Murakumo T, Koizumi Y (2004) Strengthening by γ/γ' interfacial dislocation networks in TMS-162 toward a fifth-generation single-crystal superalloy. Metallurgicals and Materials Transactions A 35(6): 1911-1914.
24. Yeh AC, Tin S (2005) Effects of Ru and Re additions on the high temperature flow stresses of Ni-based single crystal superalloys. Scripta Materialia 52(6): 519-524.
25. Shu DL, Tian SG, Tian N, Liu LR, Liang Sh, et al. (2017) Influence of Re/Ru on concentration distribution in the γ/γ' phases of nickel-based single crystal superalloys. Materials and Design 132: 198-207.
26. Mott N F, Proc. Conf (1956) on creep and fracture of metals at high temperature (C) 21.
27. Shu DL, Tian SG, Liu LR, Zhang BS, Tian N (2018) Elements distribution and deformation features of a 4.5%Re nickel-based single crystal superalloy during creep at high temperature. Materials Characterization 141: 433–441.
28. Larson DJ, Wissman BD, Martens RL (2001) Advances in atom probe specimen fabrication from planar multilayer thin film structures. Microscopy & Microanalysis 7(1): 24-31.
29. Yu XX, Wang CY, Zhang XN (2014) Synergistic effect of rhenium and ruthenium in nickel-based single-crystal superalloys. Journal of Alloys and Compounds 582: 299-304.
30. Yan HJ, Tian SG, Zhao GQ (2019) Deformation features and affecting factors of a Re/Ru-containing single crystal nickel-based superalloy during creep at elevated temperature. Materials Science & Engineering A 768: 138437.

DOI: 10.32474/ARME.2022.03.000173